



**HAL**  
open science

## Theoretical study of low-lying electronic states of AgH including spin-orbit coupling

Weiqi Zhou, Yujie Zhao, Guqing Guo, Xiaohu He, Ting Gong, Xuanbing Qiu, Yali Tian, Xiaochong Sun, Shuping Liu, Jianghui Cai, et al.

► **To cite this version:**

Weiqi Zhou, Yujie Zhao, Guqing Guo, Xiaohu He, Ting Gong, et al.. Theoretical study of low-lying electronic states of AgH including spin-orbit coupling. *Journal of Molecular Structure*, 2023, 1286, pp.135524. 10.1016/j.molstruc.2023.135524 . hal-04248383

**HAL Id: hal-04248383**

**<https://hal.science/hal-04248383v1>**

Submitted on 18 Oct 2023

**HAL** is a multi-disciplinary open access archive for the deposit and dissemination of scientific research documents, whether they are published or not. The documents may come from teaching and research institutions in France or abroad, or from public or private research centers.

L'archive ouverte pluridisciplinaire **HAL**, est destinée au dépôt et à la diffusion de documents scientifiques de niveau recherche, publiés ou non, émanant des établissements d'enseignement et de recherche français ou étrangers, des laboratoires publics ou privés.

# Theoretical Study of Low-Lying Electronic States of AgH including Spin-Orbit Coupling

Weiqi Zhou<sup>a</sup>, Yujie Zhao<sup>a</sup>, Guqing Guo<sup>a</sup>, Xiaohu He<sup>a</sup>, Ting Gong<sup>a</sup>, Xuanbing Qiu<sup>a</sup>, Yali Tian<sup>a</sup>,  
Xiaochong Sun<sup>a</sup>, Shuping Liu<sup>a</sup>, Jianghui Cai<sup>a</sup>, Béla Fiser<sup>b,c</sup>, Milán Szóri<sup>b</sup>, Christa Fittschen<sup>d</sup>, and  
Chuanliang Li<sup>a,d,\*</sup>

<sup>a</sup> Shanxi Engineering Research Center of Precision Measurement and Online Detection Equipment and School of Applied Science, Taiyuan University of Science and Technology, Taiyuan 030024, China

<sup>b</sup> Institute of Chemistry, University of Miskolc, Miskolc-Egyetemváros A/2, H-3515 Miskolc, Hungary

<sup>c</sup> Ferenc Rakoczi II Transcarpathian Hungarian College of Higher Education, 90200 Beregszász, Transcarpathia, Ukraine

<sup>d</sup> Université Lille, CNRS, UMR 8522 - PC2A - Physicochimie des Processus de Combustion et de l'Atmosphère, Lille F-59000, France

## HIGHLIGHTS:

1. The PECs of the 6  $\Lambda$ -S states have been calculated.
2. The PECs of the 11  $\Omega$  states arising from 6  $\Lambda$ -S states have been calculated.
3. TDM of spin forbidden transition from different multiplicity were investigated.
4. Interference of the intermediate  $a'^3\Sigma^+$  on direct laser cooling has been studied.

---

\* Corresponding author

E-mail: [elli@tyust.edu.cn](mailto:elli@tyust.edu.cn)

## Abstract

High-level *ab initio* calculation of silver hydride (AgH) is performed by utilizing the internally contracted multi-reference configuration interaction plus Davidson correction method. A total of 6  $\Lambda$ -S states and 11  $\Omega$  states from low-lying electronic states are computed in consideration of the spin-orbit coupling (SOC). The spectroscopic constants of bound states are determined and are in good agreement with the results of the available literatures. A large aug-cc-pwCV5Z-PP basis set for Ag atom is applied during the calculations. The transition dipole moment (TDM) of spin forbidden transition between different multiplicity, caused by SOC effect, are computed based on Breit-Pauli operator. Particularly, the TDM of spin forbidden transition between triplet  $a^3\Sigma^+$ ,  $a^3\Pi$ ,  $b^3\Sigma^+$  and singlet  $X^1\Sigma^+$ ,  $A^1\Sigma^+$ ,  $C^1\Pi$  is studied and discussed. Finally, the interference of laser directly cooling by intermediate  $a^3\Sigma^+$  states due to SOC was investigated according to numerically solving rate equations based on the obtained TDM parameters. It proves that the perturbation from  $a^3\Sigma^+$  state could be neglected in the laser cooling process.

*Keywords:* AgH, *ab initio* calculation, spectroscopic parameters, spin-orbit coupling, laser cooling

## 1. Introduction

Heavy metal hydrides are multipotent species which can act as important chemical intermediates in catalytic process [1-3], vital energy materials in fuel cell [4], and their spectra are of significant interest in astrophysics, since they are evidently observed in cool stars and brown dwarfs [5]. AgH is one of the typical heavy metal hydrides, and thus, it serves as a good example for studying the relativistic effects on the electronic structure [6].

AgH has been the vigorous subject of spectroscopic investigations from its first observation in 1925 [7]. Subsequently, Hulthén and Zumstein analyzed its rotationally resolved UV/visible spectra [8]. In 1931 Bengtsson and Olsson recorded an emission lines of AgH and observed 27 bands of  $A^1\Sigma-X^1\Sigma^+$  system [9]. Later, Hulthen and Knave observed the transition of the  $A-X$  system of the AgH isotope AgD in 1935 [10], but they only reported the rotational constants of the energy levels. Then the  $A-X$  system for AgH was analyzed in detail by Gerö and Schmid in 1943 [11]. They recorded and observed 60 bands of AgH, revealing a distinct anomalous  $A^1\Sigma^+$  state. Based on the irregular behaviors, they proposed that it was mainly caused by the perturbation from the nearby  $B^1\Sigma^+$  state. Two decades later, R. C. M. Learner put forward different opinions on Gerö and Schmid's explanation of the anomalous behavior of  $A^1\Sigma^+$  state [12], and he proposed that the anomalous shape of  $A^1\Sigma^+$  state was the result of the avoidance of crossover. Finally, the first high resolution spectroscopy experiment was a considerable improvement in accuracy by Birk and Jones in 1989 [13]. They measured the infrared spectra of two isotopologues, namely  $^{107}\text{AgH}$  and  $^{109}\text{AgH}$ , by using a tunable diode laser spectrometer.

For heavy metal hydride molecules, relativistic effects must be considered during *ab initio* calculations of equilibrium bond lengths, dissociation energies, and dipole moments. In the 1970s, AgH was taken as the prototype for studying relativistic effects in diatomic species [14, 15]. However, most similar studies focused on the ground state of AgH [16-21]. Witek *et al.* [22] studied the ground state  $X^1\Sigma^+$  and the first few excited states of AgH. The potential energy curve (PEC) of the  $A^1\Sigma^+$  state of AgH was calculated by using relativistic all-electron multi-reference perturbation, but the results are not perfectly consistent with those of Learner [12]. It was shown that there is a change in the curve at the bond length around 3 Å. Witek *et al.* [23] utilized the second-order multistate multireference perturbation theoretical calculations, including spin-orbit coupling (SOC) effect and relativistic effects, to explain that the peculiar shape of the  $A^1\Sigma^+$  due to the two avoided crossings. Li *et al.* [24] used the relativistic effective nuclear potential of Ag to evaluate the elements of the SO interaction matrix between  $^1\Sigma^+$  and  $^3\Pi$  states and the non-adiabatic coupling states between  $^1\Sigma^+$  states. Regarding the low-lying states and SOC effects, the accurate calculations of electronic structure and spectroscopic properties of AgH still remain sparse. The SOC effect dominates the complex electronic structure of open-shell diatomic systems, in particular, those containing a transition metal [25]. In addition, the SOC interaction not only changes the radiative, magnetic, and electrical properties of the excited state, but also makes possible inter-combination (spin-forbidden) transitions, self-ionization, and dissociative recombination.

Furthermore, AgH is an important candidate for laser cooling. Guided by the laser cooling criteria [26], schemes for cooling many diatomic neutrals have been proposed, such as RaF [27], AlH [28], AlF [28], BeF [29], MgF [30], GaF [31], and BH [31]. Experimentally, significant

progress has been made over the past decade in direct laser cooling and magneto-optical trapping of diatomic molecules including SrF [32], YO [33, 34], and CaF [35, 36]. As for AgH, we proposed the simplest  $^1\Sigma\text{-}^1\Sigma$  electronic system of direct laser cooling [37]. It is worth noting that the ground triplet state ( $a^3\Sigma^+$ ), the only intermediate electronic state between the  $X^1\Sigma^+$  and  $A^1\Sigma^+$  states, is weakly bound, which potentially poses an additional channel for population leakage in laser cooling. To achieve a high cooling efficiency, spontaneous decays from states involved in the closed-cycle transitions out of the cycle should be avoided.

The aims of this work are to carry out internally contracted multiconfiguration-reference configuration interaction (MRCI) calculations to predict molecular constants and transition properties of AgH relevant to SOC. The 6  $\Lambda\text{-S}$  states split into 11  $\Omega$  states when the SOC is considered, and the spectroscopic constants of low-lying  $\Lambda\text{-S}$  and the corresponding  $\Omega$  states are obtained based on the computed PECs. Besides acquiring the transition dipole moment (TDM) between singlet and triplet states, the influence of intermediate  $^3\Sigma$  state is considered in the  $^1\Sigma\text{-}^1\Sigma$  transition system for the direct laser cooling of AgH.

## 2. Methods and Computational details

The *ab initio* calculations of the electronic structure of the AgH were performed by using the complete active space self-consistent field (CASSCF) followed by the MRCI approach [38-40]. All in all, 69 single point energy calculations were carried out for each state in the internuclear distance ( $R$ ) range 0.8Å - 8.0Å to construct the PECs. The correlation consistent basis sets aug-cc-pwCVnZ-PP ( $n = T, Q, \text{ and } 5$ ) for 4*d* and 5*d* metals [41-43] were employed, with correspondence to pseudopotential for the inner core electrons. The core electrons of the Ag atom are represented by the energy-consistent pseudo-potential [44], which is formed from the basis set converged toward the complete basis set limit [41]. The PP replaces 28 electrons of 1s – 3d cores of Ag. The 28 electrons of inner shell in the Ag atom are not removed and are treated as a single nucleus, and the aug-cc-pwCV5Z-PP [41] and aug-cc-pV5Z [45] basis sets were selected for the Ag atom and the H atom, respectively. The  $C_{2v}$  point group was adopted in the calculation of electronic structures. The  $C_{2v}$  point group, as a sub-group of the  $C_{\infty v}$  point group, holds A1/A2/B1/B2 irreducible representations and the corresponding relationships between the  $C_{\infty v}$  and  $C_{2v}$  point groups are  $\Sigma^+=A_1$ ,  $\Pi=B_1+B_2$ ,  $\Delta=A_1+A_2$  and  $\Sigma^-=A_2$  respectively. For the AgH molecule, five a1, one b1, one b2, and one a2 molecular orbitals (MOs) were chosen as the active space, corresponding to the atom orbitals of 4d, 5s, and 5p $\sigma$  for Ag and 1s for H. Therefore, the active space is denoted as (5, 1, 1, 1), which represents 12 electrons occupying 8 MOs. Additionally, the 4s and 4p orbitals of Ag are closed but are not frozen in the calculations.

In MRCI calculation, all configuration state functions in CASSCF were taken as a reference. All electrons are correlated. The calculations were carried out in restriction of the  $C_{2v}$  point group by using the MOLPRO program suite [46]. The spin-orbit coupling terms were evaluated between the electronic states of interest over the CASSCF wavefunctions and the Breit-Pauli Hamiltonian. The 6  $\Lambda\text{-S}$  states split into 11  $\Omega$  states in consideration of the SOC effect. The PECs of these 6  $\Lambda\text{-S}$  and 11  $\Omega$  states were derived based on the avoided crossing rule.

According to the PECs of the  $\Lambda\text{-S}$  and  $\Omega$  states, the corresponding spectroscopic constants of the bound states, including equilibrium internuclear distance  $R_e$ , vibrational constants  $\omega_e$ , and  $\omega_e x_e$ , and rotation constant  $B_e$ , centrifugal distortion constant  $D_e$ , were determined by solving the one-

dimensional nuclear Schrödinger equation with the aid of the LEVEL program [47, 48]. The transition properties of the AgH between different multiplicities caused by SOC were also evaluated at the MRCI level. Finally, the interference of SOC on direct cooling of laser intermediate states was investigated by numerically solving the rate equation using the obtained TDM parameters.

### 3. Result and Discussion

#### 3.1 PECs and spectroscopic constants of $\Lambda$ -S states

PECs as a function of internuclear distance are plotted in Figure 1. The energy of these potentials is given with respect to the minimum of ground state  $X^1\Sigma^+$ . Six  $\Lambda$ -S states including three singlet states ( $X^1\Sigma^+$ ,  $A^1\Sigma^+$ , and  $C^1\Pi$ ) and three triplet states ( $a'^3\Sigma^+$ ,  $a^3\Pi$ , and  $b'^3\Sigma^+$ ) were calculated. These electronic states are associated with converge adiabatic to the  $\text{Ag}(^2S_g) + \text{H}(^2S_g)$  and  $\text{Ag}(^2P_u) + \text{H}(^2S_g)$  asymptotes. Generally, the pattern of the electronic states located in the Franck–Condon region is in good agreement with the previous ones. At its equilibrium, the ground ( $X^1\Sigma^+$ ) state arises mainly from the configuration of  $10\sigma^2 11\sigma^2 5\pi_x^2 5\pi_y^2 2\delta^2 12\sigma^2 13\sigma^0 14\sigma^0$  (96.92%). The first ( $A^1\Sigma^+$ ) and the lowest triplet electronic state ( $a'^3\Sigma^+$ ) are generated by the promotion of an electron from the  $12\sigma$  orbitals to the  $13\sigma$  orbital. The specific electronic configuration of all states is listed in the Table 1. It is noted that the ground triplet ( $a'^3\Sigma^+$ ) state, the only intermediate electronic state between the  $X^1\Sigma^+$  and  $A^1\Sigma^+$  states, is weakly bound. Its PEC features a shallow well and does not hold any vibrational levels according to the calculation. PECs of the other two triplet states ( $a^3\Pi$  and  $b'^3\Sigma^+$ ) almost overlap with the  $C^1\Pi$  state.

**Table 1.** The main configurations at  $R_e$  of the  $\Lambda$ -S States of AgH

$\Lambda$ -S States	Main configurations at $R_e$ (%)
$X^1\Sigma^+$	$10\sigma^2 11\sigma^2 5\pi_x^2 5\pi_y^2 2\delta^2 12\sigma^2 13\sigma^0 14\sigma^0$ (96.92%)
$A^1\Sigma^+$	$10\sigma^2 11\sigma^2 5\pi_x^2 5\pi_y^2 2\delta^2 12\sigma^1 13\sigma^1 14\sigma^0$ (67.66%)
$a'^3\Sigma^+$	$10\sigma^2 11\sigma^2 5\pi_x^2 5\pi_y^2 2\delta^2 12\sigma^2 13\sigma^0 14\sigma^0$ (18.63%)
$C^1\Pi$	$10\sigma^2 11\sigma^2 5\pi_x^1 5\pi_y^2 2\delta^2 12\sigma^2 13\sigma^1 14\sigma^0$ (69.67%)
$a^3\Pi$	$10\sigma^2 11\sigma^2 5\pi_x^2 5\pi_y^1 2\delta^2 12\sigma^2 13\sigma^1 14\sigma^0$ (98.93%)
$b'^3\Sigma^+$	$10\sigma^2 11\sigma^1 5\pi_x^2 5\pi_y^2 2\delta^2 12\sigma^2 13\sigma^1 14\sigma^0$ (98.83%)

The calculated spectroscopic constants are listed in Table 2. The equilibrium distance of the ground state  $X^1\Sigma^+$  is calculated at 1.618 Å, which is close to the experimental value of Bengtsson and Olsson [9]. Compared with the Bengtsson's work as listed in Table 2, the differences with our determined  $B_e = 6.448\text{cm}^{-1}$ ,  $\omega_e = 1746.47\text{cm}^{-1}$ , and  $\omega_e\chi_e = 38.89\text{cm}^{-1}$ , are  $0.002\text{cm}^{-1}$ ,  $13.23\text{cm}^{-1}$ , and  $4.92\text{cm}^{-1}$ , respectively. As aforementioned, the shallow potential well of the lowest triplet ( $a'^3\Sigma^+$ ) state does not hold vibrational levels, so the constants of this continuum state are not derived. The following spectroscopic parameters for  $A^1\Sigma^+$  state such as,  $R_e = 1.614\text{Å}$ ,  $B_e = 6.448\text{cm}^{-1}$ ,  $D_e = 2.23\text{eV}$  agree well with those obtained by Witek and coworkers [22]. The calculated  $T_e$  and  $\omega_e\chi_e$  for the state  $C^1\Pi$  are  $44966\text{cm}^{-1}$  and  $43\text{cm}^{-1}$ , the corresponding experimental values are

41261  $\text{cm}^{-1}$  and 42  $\text{cm}^{-1}$  [49]. Therefore, the deviations are 8% and 2.4%, respectively. Although  $D_e$  of state  $a^3\Pi$  is close to the experimental value of 1.2 eV, the consistence of  $B_e$  and  $\omega_e$  with experimental ones are not perfect [49]. The  $T_e$  value of state  $A^1\Sigma^+$  is 29989  $\text{cm}^{-1}$ , close to the experimental value 29959  $\text{cm}^{-1}$  [49]. For state  $C^1\Pi$  and state  $a^3\Pi$ , the differences with the experimental values are with 8.9% and 1.9% errors, respectively [49].

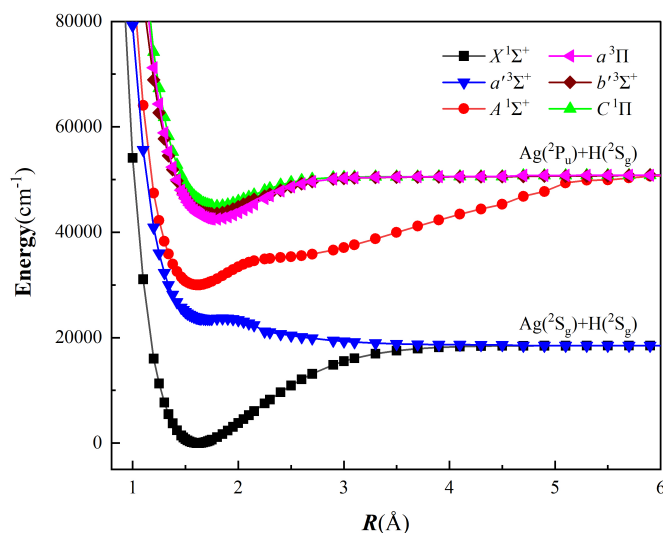


**Fig.1.** Calculated potential energy curves (PECs) of  $\Lambda$ -S states of AgH

**Table 2.** Spectroscopic constants of  $\Lambda$ -S states of AgH

$\Lambda$ -S States	$T_e(\text{cm}^{-1})$	$R_e(\text{\AA})$	$B_e(\text{cm}^{-1})$	$D_e(\text{eV})$	$\omega_e(\text{cm}^{-1})$	$\omega_e x_e(\text{cm}^{-1})$	Ref.
$X^1\Sigma^+$	0	1.618	6.448	2.29	1746.47	38.89	This work
	0	1.6177	6.44647	2.16	1634.2	35.32	Cal.[37]
		1.62	6.43		1902		Cal.[22]
		1.6174	6.499	2.38	1759.9	34.18	Cal.[50]
$A^1\Sigma^+$		1.6172	6.45		1759.7	33.97	Exp.[9]
	29989	1.614	6.448	2.23	1791.94	47	This work
	29500	1.6412	6.263	2.34	1659.7	122	Cal.[37]
$C^1\Pi$		1.604	6.56		1805		Cal.[22]
	29959	1.638	6.265	2.36	1663.6	87	Exp.[49, 51]
	44966	1.79	5.24	0.72	1425	43	This work
	41274	1.7875	5.28	0.63	1477	69	Cal.[37]
$a^3\Pi$	41261	1.6	6.54		1589	42	Exp.[49]
	42502	1.77	5.37	1.03	1524	36.4	This work
	38601	1.7626	5.43	0.96	1502	21.1	Cal.[37]
	44305	1.594	6.644	0.91	1620	89.4	Cal.[52]
		1.594	6.64		1742		Cal.[22]
$b^3\Sigma^+$	41700	<1.64	>6.3	1.20	1450	50	Exp.[49]
	43483	1.75	5.45	0.56	1475	29	This work
	39743	1.7466	5.53	0.82	1603	103	Cal.[37]

### 3.2 Spin-orbit coupling of the $\Lambda$ -S states

The SOC effect is the main source of intramolecular perturbations due to the flexible selection rules for the corresponding SO operator. Typically, the strength of the SO interaction decreases as electronic excitation energy increases. However, the impact of this interaction on the nonadiabatic mixing of excited states does not diminish, since the density of interacting states grows rapidly at highly excited states.

To elucidate the strong interactions between the electronic states of AgH, we calculate the SOC matrix elements  $|H_{\text{so}}|$  of the  $\Lambda$ -S states with Breit-Pauli operators. Figure 2 presents the calculated  $|H_{\text{so}}|$  results as a function of the internuclear distance, as shown the SOC of  $X^1\Sigma^+ - a^3\Pi$ ,  $A^1\Sigma^+ - a^3\Pi$ ,  $C^1\Pi - a^3\Sigma^+$ ,  $C^1\Pi - b^3\Sigma^+$ ,  $a^3\Sigma^+ - a^3\Pi$  and  $b^3\Sigma^+ - a^3\Pi$ . The  $|H_{\text{so}}|$  in the Franck-Condon region ( $R_e$  of  $X^1\Sigma^+$  is 1.618 Å) is in the range of -1100 ~800  $\text{cm}^{-1}$ . At the crossing points between the  $\Lambda$ -S states, the  $|H_{\text{so}}|$  values are about 590, 549 and 140  $\text{cm}^{-1}$  for  $A^1\Sigma^+ - a^3\Pi$ ,  $b^3\Sigma^+ - a^3\Pi$  and  $a^3\Sigma^+ - a^3\Pi$  respectively. These results strongly indicate that the SOC effect plays an important role in electronic states of AgH. The SOC effect will lead to the splitting of multiplet electronic states and strong interactions for the  $\Lambda$ -S states of the molecules. In consideration of SOC,  $X^1\Sigma^+$  corresponds to  $X0^+$  state,  $A^1\Sigma^+$  becomes to  $(2)0^+$  state,  $a^3\Sigma^+$  splits to  $(1)0^-$  and  $(1)1$  states,  $b^3\Sigma^+$  corresponds to  $(3)0^-$  and  $(3)1$  states,  $a^3\Pi$  splits to  $(2)0^-$ ,  $(1)2$ ,  $(2)1$  and  $(3)0^+$  states, and  $C^1\Pi$  respects to  $(4)1$  state. Consequently, the PECs as well as the spectroscopic constants and transition properties for the corresponding states will be affected as will be discussed in detail in the following section.

The SO functions themselves are strongly dependent on internuclear distance  $R$ , and their long-range tails are responsible for the complex dynamics of states near the dissociation threshold. The main component of the ground state  $X0^+$  in the  $R=0.8 - 8.0\text{\AA}$  region comes from the  $X^1\Sigma^+$  state. For the ground state, the effect of SOC is small and can be neglected. For either  $(1)0^-$  or  $(1)1$  state, the  $a^3\Sigma^+$  state is the leading component, but a trace partition of  $a^3\Pi$  state is found, accounting for about 0.1%-0.3%. As examples, the  $\Lambda$ -S compositions of  $(2)0^+$ ,  $(2)0^-$ ,  $(3)1$ , and  $(3)0^-$  states are stated as follows. The main component of  $(2)0^+$  state is 99.98%  $A^1\Sigma^+$  state at  $R\sim 0.9\text{\AA}$ , and  $a^3\Pi$  participates with the increase of bond length. The composition of  $(3)1$  state finally consists of 60.43%  $A^1\Sigma^+$  state and 39.56%  $a^3\Pi$  state at  $R>2.3\text{\AA}$ . With the increase of  $R$ , the composition of the  $(3)1$  state contains not only the  $b^3\Sigma^+$  state, but also the  $C^1\Pi$  and  $a^3\Pi$  states.

Although the four electronic states are dominated by  $A^1\Sigma^+$ ,  $b^3\Sigma^+$ , and  $a^3\Pi$ , respectively, there will be disturbances of other  $\Lambda$ -S states at large  $R$  region, indicating the complicated state-mixing and interaction between the excited electronic states of AgH.

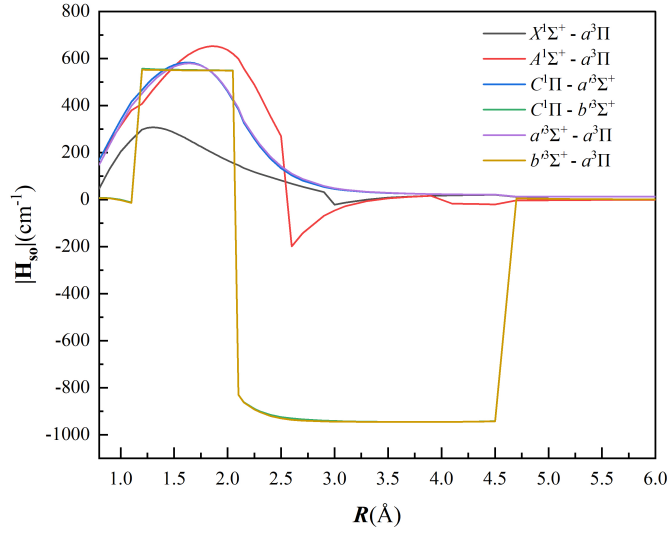


**Fig.2.** The spin-orbit matrix elements of  $\Lambda$ -S states of AgH

**Table 3.** Dissociation limit relationships of  $\Omega$  states of AgH

$\Omega$ states	Atomic state (Ag+H)	Energy( $\text{cm}^{-1}$ )	
		Calc.	Expt. [53]
X0+, (1)0-, (1)1	Ag( $^2S_{1/2}$ ) + H( $^2S_{1/2}$ )	0	0
(2)0+, (2)0-, (2)1	Ag( $^2P_{1/2}$ ) + H( $^2S_{1/2}$ )	29272	29552
(3)0+, (3)0-, (3)1, (4)1, (1)2	Ag( $^2P_{3/2}$ ) + H( $^2S_{1/2}$ )	30494	30242

### 3.3 PECs and spectroscopic constants of $\Omega$ states

Figure 1 shows the high density of electronic states located for energies greater than  $40000 \text{ cm}^{-1}$ . This high density should favor their mutual interactions and the mixings of their wavefunctions by vibronic, SO, and rotational couplings. The  $\Lambda$ -S states are split into their spin-orbit components with a definitive  $\Omega$  quantum number. In the present work, we consider three states of  $0+$ , three states of  $0-$ , four states of  $1$ , and one state of  $2$  due to SOC. The  $\Omega = 0+$  states arise from the  $X^1\Sigma^+$ ,  $A^1\Sigma^+$  and  $a^3\Pi$  states, the  $\Omega = 0-$  states are from the  $a^3\Sigma^+$ ,  $b^3\Sigma^+$  and  $a^3\Pi$  states, and the  $\Omega = 1$  states origin from  $C^1\Pi$ ,  $a^3\Sigma^+$ ,  $b^3\Sigma^+$  and  $a^3\Pi$  states. The  $\Omega = 2$  state arises from the  $a^3\Pi$  state. These  $\Omega$  states correspond to three dissociation limits and are tabulated in Table 3. These  $\Omega$  states correspond to three dissociation limits. The detailed dissociation relationships of the  $\Omega$  states are listed in Table 3. The calculated the dissociation limits are in good agreement with the experimental values [53], and the corresponding difference values are  $280\text{cm}^{-1}$  and  $252\text{cm}^{-1}$ . In Figure 3, it shows the calculated PECs of the  $\Omega$  states of AgH. In Figure 4, it shows the PECs from Figure 3 separated according to different  $\Omega$  substate. Figure (a), (b), (c) and (d) of Figure 4 all contain the ground state X0+ for comparison. From the PECs of the bound  $\Omega$  states, the spectroscopic constants are obtained, and the corresponding results are presented in Table 4.

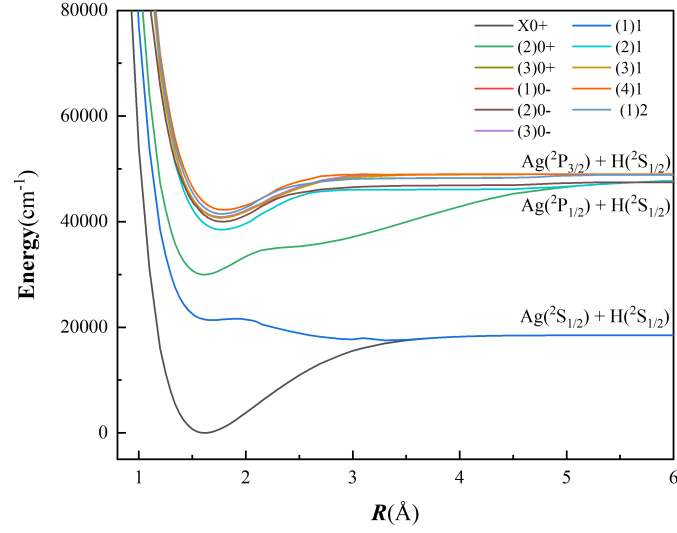


**Fig.3.** Calculated potential energy curves (PECs) of  $\Omega$  states of AgH

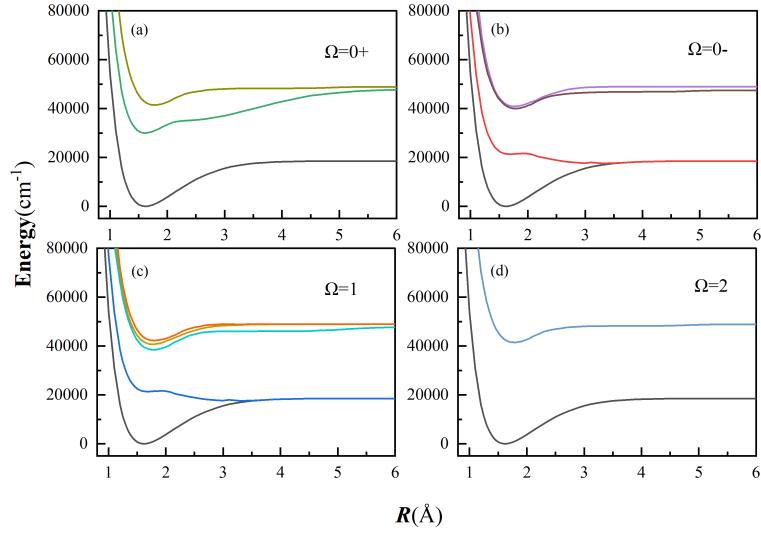


**Fig.4.** (a) PECs from Fig. 3 for  $\Omega = 0+$ , (b) PECs from Fig. 3 for  $\Omega = 0-$ , (c) PECs from Fig. 3 for  $\Omega = 1$ , (d) PECs from Fig. 3 for  $\Omega = 2$ .

**Table 4.** Computed spectroscopic constants of  $\Omega$  states of AgH along with literature data

$\Omega$ States	$T_e(\text{cm}^{-1})$	$R_e(\text{Å})$	$B_e(\text{cm}^{-1})$	$D_e(\text{eV})$	$\omega_e(\text{cm}^{-1})$	$\omega_e x_e(\text{cm}^{-1})$	Ref.
X0+	0	1.618	6.45	2.29	1746	38.89	This work
	0	1.620	6.43		1902		Cal.[22]
	0	1.618	6.45	2.38979	1760	34	Exp.[54]
(2)0+	29989	1.6138	6.45	2.233	1792	47	This work
	29195	1.604	6.56		1805		Cal.[22]
	29921	1.665	6.09	2.368	1490	87	Exp.[54]
(4)1	42233	1.8	5.2	0.84	1440	11.57	This work
	46696	1.934	4.51		1028		Cal.[22]
	46696	1.8	5.23		845		Exp.[54]
(1)2	41489	1.779	5.32	0.91	1523	31.24	This work

	42018	1.584	6.73		1662		Cal.[22]
	41700	<1.64	>6.3		1450		Exp.[54]
(2)1	40504	1.7712	5.36	1.03	1487	31.54	This work
	43389	1.814	5.13		1326		Cal.[22]
		1.875	4.81				Exp.[54]
(3)0+	41490	1.779	5.33	0.91	1524	31.19	This work
	43184	1.549	6.64		1742		Cal.[22]
	41696	<1.64	>6.3		1450		Exp.[54]
(3)1	40739	1.7801	5.33	1.11	1502	37.44	This work
	42745	1.604	6.56		1120/1581		Cal.[22]
	41212	1.61	6.54		1589	42	Exp.[54]

There are several avoided crossings induced by the strong SOC between the states. Because of the SOC effect, the shape of a  $\Omega$ -state PEC changes significantly comparing to the corresponding  $\Lambda$ -S states. As listed in Table. 4, the molecular constants of X0+ state from this work is in agreement with the experimental values [54]. The  $\omega_e$  and  $\omega_e\chi_e$  have a difference of 14  $\text{cm}^{-1}$  and 4.89  $\text{cm}^{-1}$ , respectively. The  $a^3\Pi$  state is split into (1)2, (2)1 and (3)0+ substates due to spin-orbit coupling. Our calculated results basically agree with the experimental values [54], although the  $\omega_e$  of (1)2, (3)0+ states are overestimated by 64  $\text{cm}^{-1}$  and 74  $\text{cm}^{-1}$ ,  $R_e$  of (2)1 state is underestimated by 0.1038 Å and its  $B_e$  is overestimated by 0.55 eV. Meanwhile, it is discovered that SOC effect significantly influences the calculated results of PECs for heavy metal hydride molecules, so it could not be ignored.

### 3.4 Transition moment of spin forbidden transition between different multiplicity

For a diatomic heteronuclear molecular system, the selection rules are  $\Delta\Lambda=0,\pm 1$ ;  $\Delta S=0$ ;  $\Delta\Sigma=0$ ;  $\Delta\Omega=0,\pm 1$  [55]. Obviously, from the above selection rule, the transition with  $\Delta S=1$  is forbidden. However, it could make inter-combination (spin-forbidden) transitions possible due to SOC [56, 57]. The triplet states and singlet state  $C^1\Pi$  of AgH, where the electronic states are in close proximity on the potential energy curves. These triplets connect the singlets located in the Franck-Condon region of the ground state to the corresponding photodissociation products. For AgH ( $C^1\Pi$ ), the situation is complicated since this singlet is embedded into a set of potentials of the triplets. Currently, we consider the transition properties between the different multiplicity states.

Figures 5 and 6 illustrate the calculated transition moments as the functions of internuclear distances for the transitions between the singlet and triplet states. Figure 5 (a) depicts that the transition moment  $\langle(3)1|\mu|X0+\rangle$  is as large as 0.35 D in comparison with 0.039 D for  $\langle(1)1|\mu|X0+\rangle$  around  $R_e$ . The transition moment of  $\langle(2)1|\mu|X0+\rangle$  shares the similar trend with that of  $\langle(3)1|\mu|X0+\rangle$  at  $R=1.5$  Å-1.8 Å, but its value 0.277 D is smaller. Additionally, the  $\langle(1)1|\mu|X0+\rangle$  varies little in the Franck-Condon region. In the range of 2.1 Å – 3.5 Å, the TDM of spin forbidden transition between  $b^3\Sigma^+$ ,  $a^3\Pi$  and  $X^1\Sigma^+$  decreases with the increase of  $R$ . For the transition moment of  $\langle(2)1|\mu|X0+\rangle$ , it reaches the maximum at 2.05 Å and gradually tends to zero at 3.5 Å, indicating that no transition occurs later. Corresponding to the potential energy curve, 3.5 Å is exactly the edge of the potential well for (2)1 and X0+ states.

As presented in Figure 5 (b), the transition moment of triplet  $\Omega$ -states with (2)0+ is much smaller than that of interaction with X0+, in between 0.0 and 0.1 a.u., therefore their relevance is

minor. The tendency of the TDM of spin forbidden transition between (2)1, (3)1 and (2)0+ is generally identical to each other.

Eight  $\Omega$ -states could interact with (4)1 state according to the transition selection rules. The topography of transition moment with internuclear distance of  $\langle(1)1|\mu|(4)1\rangle$  and  $\langle(2)1|\mu|(4)1\rangle$  are comparable and their maximum occurs around 2.1Å and 2.6 Å. However, the maximum magnitude of the transition moment corresponding to (1)1, shown in Figure 6(a), is 3.6 times more than that of the  $\langle(2)1|\mu|(4)1\rangle$  presented in Figure 6(b). Transition moments from other  $\Omega$ -states with (4)1 state too weak to be neglected for electronic transitions.

Thus, the AgH molecule has an intermediate state  $a'^3\Sigma^+$  between the ground state  $X^1\Sigma^+$  and the first excited state  $A^1\Sigma^+$ . Further question is that the intermediate state would terminate the laser cooling cycle of the  $^1\Sigma$ - $^1\Sigma$  electronic transition, because the spontaneous radiation of  $A^1\Sigma^+ - a'^3\Sigma^+$  arises from the TDM of spin forbidden transition and  $a'^3\Sigma^+$  is a dissociative state. The lost number of molecules in laser cooling was acquired by Einstein coefficient. In combination with the TDM of spin forbidden transition, Einstein coefficient of spontaneous emission between bound and dissociative state was calculated via BCONT program [58]. The result shows it is as small as 0.136 for  $A^1\Sigma^+(v'=0, J'=0) - a'^3\Sigma^+$ . With comparison of  $1.79 \times 10^7$  for  $A^1\Sigma^+(v'=0, J'=1) - X^1\Sigma^+(v''=0, J''=0)$ , the lost molecules due to intermediate  $a'^3\Sigma^+$  state could be neglected in laser cooling process.

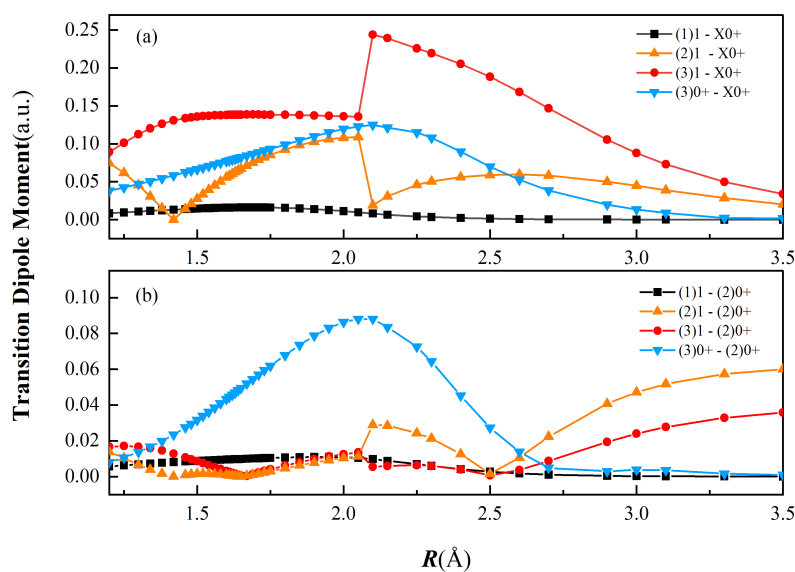


**Fig.5.** (a) Transition pole moment of (1)1, (2)1, (3)1 and (3)0+ with  $X^0+$ , (b) Transition pole moment of (1)1, (2)1, (3)1 and (3)0+ with  $(2)0+$ .

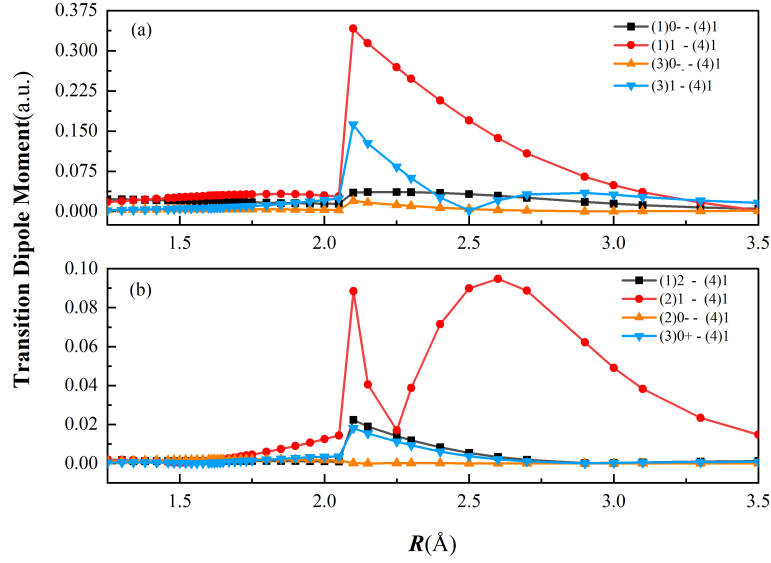


**Fig.6.** (a) Transition pole moment of (1)0-, (1)1, (3)0- and (3)1 with (4)1, (b) Transition pole moment between (1)2, (2)1, (2)0- and (3)0+ with (4)1.

#### 4. Conclusion

In this work, high-level *ab initio* calculations were performed on low-lying electronic states of AgH using the internally contracted MRCI method based on a large augmented correlation consistent aug-cc-pwCV5Z-PP basis sets in conjunction with effective core potentials. It was found that the intermediate state  $a^3\Sigma^+$  exists with potential wells, and its PECs holds only three vibrational levels according to the calculation. Considering the SOC, 11  $\Omega$  states generated from the 6  $\Lambda$ -S states have been studied and the corresponding molecular constants have been derived. The obtained spectroscopic parameters are consistent with the experimental ones. Maximum of transition moments for  $\langle (3)1|\mu|X0^+\rangle$  and  $\langle (3)0^+|\mu|(2)0^+\rangle$  are 0.62 D and 0.224 D around 2.1 Å, respectively. The tendency of transition moments of (1)1 and (3)1 with (2)0+ is generally identical to each other. Additionally, the transition moment lines of  $\langle (1)1|\mu|(4)1\rangle$  and  $\langle (3)1|\mu|(4)1\rangle$  are similar to each other, but the  $\langle (1)1|\mu|(4)1\rangle$ 's maximum is 2.1 times larger than that of the  $\langle (3)1|\mu|(4)1\rangle$ . The TDMs of  $X^1\Sigma^+$  and  $A^1\Sigma^+$  with the intermediate state  $a^3\Sigma^+$  were obtained. According to the obtained simulation results, it is demonstrated by solving the rate equation that the influence of intermediate states  $a^3\Sigma^+$  on the  $^1\Sigma^+ - ^1\Sigma^+$  system of direct laser cooling of AgH could be ignored.

#### 5. Acknowledgement

We are indebted to Prof. Wenli Zou in Northwest University of China and Prof. Robert W. Field in MIT Department of Chemistry for their helpful discussion and insightful suggestions. This work is supported by National Natural Science Foundation of China (U1810129, 52076145 & 11904252). BF and MS grateful for the support by the European Union and the Hungarian State, co-financed by the European Regional Development Fund in the framework of the GINOP-2.3.4-15-2016-00004 project, which aims to promote cooperation between higher education and industry. Further support to MS and BF has been provided by the National Research, Development and

Innovation Fund (Hungary) within the TKP2021-NVA-14 project.

## References

- [1] E. Larionov, H. Li, C. Mazet, Chem. Commun. (Camb). 50 (2014) 9816-9826. <https://doi.org/10.1039/C4CC02399D>
- [2] T. Liu, M. Guo, A. Orthaber, R. Lomoth, M. Lundberg, S. Ott, L. Hammarstrom, Nat Chem. 10 (2018) 881-887. <https://doi.org/10.1038/s41557-018-0076-x>
- [3] A. Candan, M. Kurban, Solid. State. Communications. 281 (2018) 38-43. <https://doi.org/10.1016/j.ssc.2018.07.004>
- [4] D. Chandra, (Eds.), Intermetallics for hydrogen storage, 'E-Publishing', Place, 2008, 'pp.'315-356
- [5] R.J. Le Roy, D.R. Appadoo, K. Anderson, A. Shayesteh, I.E. Gordon, P.F. Bernath, J Chem Phys. 123 (2005) 204304. <https://doi.org/10.1063/1.2064947>
- [6] T. Nakajima, T. Suzumura, K. Hirao, Chemical physics letters. 304 (1999) 271-277. [https://doi.org/10.1016/S0009-2614\(99\)00304-8](https://doi.org/10.1016/S0009-2614(99)00304-8)
- [7] E. Bengtsson, E. Svensson, Compt. Rend. 180 (1925)
- [8] E. Hulthén, R.V. Zumstein, Physical Review. 28 (1926) 13. <https://doi.org/10.1103/PhysRev.28.13>
- [9] E. Bengtsson, E. Olsson, Zeitschrift für Physik. 72 (1931) 163-176. <https://doi.org/10.1007/bf01341904>
- [10] E. Hulthén, E. Knave, The Hague, The Netherlands, 1935
- [11] L. Gerö, R. Schmid, Zeitschrift für Physik. 121 (1943) 459-487. <https://doi.org/10.1007/BF01330099>
- [12] Proceedings of the Royal Society of London. Series A. Mathematical and Physical Sciences. 269 (1997) 311-326. <https://doi.org/10.1098/rspa.1962.0179>
- [13] H. Birk, H. Jones, Chemical physics letters. 161 (1989) 27-29. [https://doi.org/10.1016/S0009-2614\(89\)87025-3](https://doi.org/10.1016/S0009-2614(89)87025-3)
- [14] J. Desclaux, P. Pyykkö, Chemical Physics Letters. 39 (1976) 300-303. [https://doi.org/10.1016/0009-2614\(76\)80080-2](https://doi.org/10.1016/0009-2614(76)80080-2)
- [15] P. Pyykkö, Journal of the Chemical Society, Faraday Transactions 2: Molecular and Chemical Physics. 75 (1979) 1256-1276. <https://doi.org/10.1039/F29797501256>
- [16] B.A. Heß, P. Chandra, Physica Scripta. 36 (1987) 412. <https://doi.org/10.1088/0031-8949/36/3/006>
- [17] K. Balasubramanian, The Journal of Chemical Physics. 93 (1990) 8061-8072. <https://doi.org/10.1063/1.459336>
- [18] C.L. Collins, K.G. Dyall, H.F. Schaefer, The Journal of Chemical Physics. 102 (1995) 2024-2031. <https://doi.org/10.1063/1.468724>
- [19] A. Mohanty, F. Parpia, Physical Review A. 54 (1996) 2863. <https://doi.org/10.1103/PhysRevA.54.2863>
- [20] T. Suzumura, T. Nakajima, K. Hirao, International journal of quantum chemistry. 75 (1999) 757-766. [https://doi.org/10.1002/\(SICI\)1097-461X\(1999\)75:4/5<757::AID-QUA42>3.0.CO;2-R](https://doi.org/10.1002/(SICI)1097-461X(1999)75:4/5<757::AID-QUA42>3.0.CO;2-R)
- [21] A. Avramopoulos, V.E. Ingamells, M.G. Papadopoulos, A.J. Sadlej, The Journal of Chemical Physics. 114 (2001) <https://doi.org/10.1063/1.1329890>
- [22] H.A. Witek, T. Nakajima, K. Hirao, The Journal of Chemical Physics. 113 (2000) 8015-8025. <https://doi.org/10.1063/1.1308554>

- [23] H.A. Witek, D.G. Fedorov, K. Hirao, A. Viel, P.-O. Widmark, *The Journal of Chemical Physics*. 116 (2002) <https://doi.org/10.1063/1.1465403>
- [24] Y. Li, H.-P. Libermann, R.J. Buenker, L. Pichl, *Chemical Physics Letters*. 389 (2004) 101-107. <https://doi.org/10.1016/j.cplett.2004.03.067>
- [25] J. Tennyson, L. Lodi, L.K. McKemmish, S.N. Yurchenko, *Journal of Physics B: Atomic, Molecular and Optical Physics*. 49 (2016) <https://doi.org/10.1088/0953-4075/49/10/102001>
- [26] M. Di Rosa, *The European Physical Journal D-Atomic, Molecular, Optical and Plasma Physics*. 31 (2004) 395-402. <https://doi.org/10.1140/epjd/e2004-00167-2>
- [27] T.A. Isaev, S. Hoekstra, R. Berger, *Physical Review A*. 82 (2010) <https://doi.org/10.1103/PhysRevA.82.052521>
- [28] N. Wells, I.C. Lane, *Phys Chem Chem Phys*. 13 (2011) 19018-19025. <https://doi.org/10.1039/c1cp21313j>
- [29] I.C. Lane, *Phys Chem Chem Phys*. 14 (2012) 15078-15087. <https://doi.org/10.1039/c2cp42709e>
- [30] S. Kang, Y. Gao, F. Kuang, T. Gao, J. Du, G. Jiang, *Physical Review A*. 91 (2015) <https://doi.org/10.1103/PhysRevA.91.042511>
- [31] Y.F. Gao, T. Gao, *Phys Chem Chem Phys*. 17 (2015) 10830-10837. <https://doi.org/10.1039/c5cp00025d>
- [32] E.S. Shuman, J.F. Barry, D.R. Glenn, D. DeMille, *Phys Rev Lett*. 103 (2009) 223001. <https://doi.org/10.1103/PhysRevLett.103.223001>
- [33] M. Yeo, M.T. Hummon, A.L. Collopy, B. Yan, B. Hemmerling, E. Chae, J.M. Doyle, J. Ye, *Phys Rev Lett*. 114 (2015) 223003. <https://doi.org/10.1103/PhysRevLett.114.223003>
- [34] M.T. Hummon, M. Yeo, B.K. Stuhl, A.L. Collopy, Y. Xia, J. Ye, *Phys Rev Lett*. 110 (2013) 143001. <https://doi.org/10.1103/PhysRevLett.110.143001>
- [35] V. Zhelyazkova, A. Cournol, T.E. Wall, A. Matsushima, J.J. Hudson, E.A. Hinds, M.R. Tarbutt, B. E. Sauer, *Physical Review A*. 89 (2014) <https://doi.org/10.1103/PhysRevA.89.053416>
- [36] B. Hemmerling, E. Chae, A. Ravi, L. Anderegg, G.K. Drayna, N.R. Hutzler, A.L. Collopy, J. Ye, W. Ketterle, J.M. Doyle, *Journal of Physics B: Atomic, Molecular and Optical Physics*. 49 (2016) <https://doi.org/10.1088/0953-4075/49/17/174001>
- [37] C. Li, Y. Li, Z. Ji, X. Qiu, Y. Lai, J. Wei, Y. Zhao, L. Deng, Y. Chen, J. Liu, *Physical Review A*. 97 (2018) <https://doi.org/10.1103/PhysRevA.97.062501>
- [38] P.J. Knowles, H.-J. Werner, *Chemical physics letters*. 115 (1985) 259-267. [https://doi.org/10.1016/0009-2614\(85\)80025-7](https://doi.org/10.1016/0009-2614(85)80025-7)
- [39] P.J. Knowles, H.-J. Werner, *Chemical physics letters*. 145 (1988) 514-522. [https://doi.org/10.1016/0009-2614\(88\)87412-8](https://doi.org/10.1016/0009-2614(88)87412-8)
- [40] H.J. Werner, P.J. Knowles, *The Journal of Chemical Physics*. 89 (1988) 5803-5814. <https://doi.org/10.1063/1.455556>
- [41] K.A. Peterson, C. Puzzarini, *Theoretical Chemistry Accounts*. 114 (2005) 283-296. <https://doi.org/10.1007/s00214-005-0681-9>
- [42] K.A. Peterson, D. Figgen, M. Dolg, H. Stoll, *J Chem Phys*. 126 (2007) 124101. <https://doi.org/10.1063/1.2647019>
- [43] D. Figgen, K.A. Peterson, M. Dolg, H. Stoll, *J Chem Phys*. 130 (2009) 164108. <https://doi.org/10.1063/1.3119665>
- [44] D. Figgen, G. Rauhut, M. Dolg, H. Stoll, *Chemical Physics*. 311 (2005) 227-244. <https://doi.org/10.1016/j.chemphys.2004.10.005>

- [45] R.A. Kendall, T.H. Dunning, R.J. Harrison, *The Journal of Chemical Physics*. 96 (1992) 6796-6806. <https://doi.org/10.1063/1.462569>
- [46] <http://webbook.nist.gov>
- [47] R.J. Le Roy, *Journal of Quantitative Spectroscopy and Radiative Transfer*. 186 (2017) 167-178.
- [48] W. Shi, C. Li, H. Meng, J. Wei, L. Deng, C. Yang, *Computational and Theoretical Chemistry*. 1079 (2016) 57-63. <https://doi.org/10.1016/j.comptc.2016.01.015>
- [49] *Proceedings of the Royal Society of London. Series A. Mathematical and Physical Sciences*. 269 (1997) 327-337. <https://doi.org/10.1098/rspa.1962.0180>
- [50] R.J. Le Roy, D.R. Appadoo, K. Anderson, A. Shayesteh, I.E. Gordon, P.F. Bernath, *J Chem Phys*. 123 (2005) 204304. <https://doi.org/10.1063/1.2064947>
- [51] T. Okabayashi, M. Tanimoto, *J Mol Spectrosc*. 204 (2000) 159-160. <https://doi.org/10.1006/jmsp.2000.8212>
- [52] H.A. Witek, D.G. Fedorov, K. Hirao, A. Viel, P.-O. Widmark, *The Journal of Chemical Physics*. 116 (2002) <https://doi.org/10.1063/1.1465403>
- [53] J.C. Pickering, V. Zilio, *THE EUROPEAN PHYSICAL JOURNAL D*. 13 (2001) 181-185. <https://doi.org/10.1007/s100530170264>
- [54] *Molecular Spectra and Molecular Structure IV-Constants of Diatomic Molecules*(1979,Huber,Herzberg)
- [55] H. Lefebvre-Brion and R. W. Field, *The Spectra and Dynamics of Diatomic Molecules* (Academic Press, San Diego, 2004)
- [56] C. Li, L. Deng, J. Zhang, X. Qiu, J. Wei, Y. Chen, *Journal of Molecular Spectroscopy*. 284 (2013) 29-32. <https://doi.org/10.1016/j.jms.2013.02.002>
- [57] C. Li, L. Deng, Y. Zhang, L. Wu, X. Yang, Y. Chen, *The Journal of Physical Chemistry A*. 115 (2011) 2978-2984. <https://doi.org/10.1021/jp111990z>
- [58] R.J.L. Roy, G.T. Kraemer, BCONT, Version 2.2. Computer program for calculating absorption coefficients, emission intensities or (Golden rule) predissociation rates. <http://leroy.uwaterloo.ca/programs.html>.